Current Applied Science and Technology Vol. 22 No. 6 (November-December 2022)

Research article

Preparation of Nanofibers of Poly (methyl methacrylate) Composited with Few-Layer-Graphene for Anticorrosion Layer

Korakot Onlaor, Boonthawee Putta, Thutiyaporn Thiwawong* and Benchapol Tunhoo

Electronics and Control System for Nanodevice Research Laboratory, College of Materials Innovation and Technology, King Mongkut's Institute of Technology Ladkrabang, Bangkok, Thailand

Received: 31 August 2021, Revised: 29 November 2021, Accepted: 28 January 2022

DOI: 10.55003/cast.2022.05.22.015

Keywords

graphene;

poly(methyl methacrylate);

corrosion;

electrospinning

Abstract

An anticorrosion layer is a significant component that prevents the corrosion process in materials. In this work, a nanofiber of poly (methyl methacrylate) composited with few-layer-graphene was prepared as an anticorrosion layer. An electrospinning process was applied to prepare composite nanofiber on a metal substrate at various concentrations of few-layer graphene. The physical properties of the composite nanofiber were investigated with field-emission scanning electron microscope, Raman spectroscopy, and contact angle measurement. The corrosion behavior was tested in an aqueous solution of 3.5% by weight of sodium chloride. It was found that a few-layer graphene concentration of 2 wt% in polymethacrylate showed the optimum anticorrosion on aluminum sheet, as observed on a Tafel graph. Compared with the uncoated metal, the coated aluminum sheet was protected against corrosion with a protection efficiency of 99.33%. The prepared materials prevented the infiltration of water and solution ions into the metal plate.

1. Introduction

In many structures, such as buildings or pipes, metallic materials are widely used. Corrosion is an important chemical process that generally occurs on metal surface, and is a major problem and economical burden for the metallic industry [1]. Corrosion can result in weight loss, low ductility, reduced mechanical strength, and reduced usage time [2]. Typically, the corrosion process of metal is unavoidable; however, some procedures can be used to restrict the corrosion reaction. Thus, the

*Corresponding author: Tel.: (+66) 3298000
E-mail: thutiyaporn.th@gmail.com

protection of corrosion plays an essential role in metallurgy technology. The use of anticorrosion techniques such as acid pickling, acid cleaning has been widely reported. Moreover, the use of corrosion inhibitors and the optimization of their use has been addressed [3]. Typically, the Tafel plot is a procedure based on a potentiodynamic polarization method that is widely used to rapidly and reliably estimate corrosion parameters [4, 5]. From the Tafel plot, the corrosion current (I_{corr}) and corrosion potential (E_{corr}) can be obtained from extrapolating of a straight line of oxidation and reduction process in the Tafel graph. Moreover, the characteristic parameters of corrosion inhibitors, such as corrosion protection efficiency, can be determined by calculation with the Tafel plot [6, 7].

Carbon-based materials are widely researched and developed family of materials. Common materials include fullerene, carbon nanotube, graphene, etc. Recently, graphene has received a lot of attention in the research due to its many advantageous properties [8]. Usually, graphene is a carbon-based family material which features sp^2 carbon atom bonding. Graphene exhibits a two-dimensional sheet structure [9]. Its advantageous properties become evident in various applications such as its use in solar cells, sensors, memory devices, and energy storage [10]. Moreover, graphene had been applied as a nanofiller in polymer matrices due to its excellent properties such as mechanical properties and large surface area [11].

In the recent past, composites of graphene and polymeric materials have become subjects of interest in anticorrosion research. It was reported that the impermeable barrier properties of graphene included impermeable barrier behavior, which could be used to prevent metal surfaces from chemical reactions with acids or gases [12]. Chen *et al*. [13] reported protecting copper and copper/nickel metal substrates using graphene thin films coated by a chemical vapor deposition process. Yu *et al*. [14] reported on the performance of nanocomposite film of polystyrene/graphene to protect steel electrodes with a protection efficiency of more than 99%. Bohm [15] reported on the hydrophobic properties of graphene with a high surface area that plays a key role in corrosion behavior.

Several processes have been reported for the preparation of composite materials such as the dip casting, spin coating, and sol-gel techniques. One of the essential techniques is an electrospinning process which delivers an electrostatically driven jet of precursor solution [16]. In this technique, the nonwoven nanofibers (NFs) can be produced with various diameters. The prepared nanofibers exhibited a high surface area to volume ratio that could be used in many applications such as sensors, energy storage, and filtration [17-19]. Typically, the hierarchically structured nanofibers that were prepared by the electrospinning process exhibited hydrophobic properties [20], which were important in the functioning of the anticorrosion layer.

Poly (methyl methacrylate) (PMMA) is a thermoplastic polymer with excellent physical properties such as good hardness, high tensile strength, and low electrical conductivity. Typically, PMMA exhibits low chemical resistance, which can be improved by chemical or physical modification [21]. Therefore, composites of graphene and PMMA seemed to be good candidates for corrosion inhibitors with a simple preparation process displaying strong adhesion onto the metallic_substrate. In this work, poly (methyl methacrylate) and few-layer-graphene (FLG) composites were prepared by the electrostatic spinning process for use as anticorrosion layers. The physical properties of composite nanofibers were investigated. The effects of FLG concentration in the composite PMMA nanofibers on anticorrosion behavior were demonstrated with electrochemical measurement, and the efficiency of corrosion protection was demonstrated.

2. Materials and Methods

2.1 Materials preparation

PMMA (average M_w ~120,000) and few-layer-graphene (FLG) powders were purchased from Aldrich Chem. Co., and Haydale Technologies Co. To prepare the precursor solution, PMMA was dissolved in acetone with a 100 mg/ml concentration. Then, FLG powders were mixed into the solution at various concentrations of 0.2, 0.50, 1.0 and 2.0% by weight, respectively. A sonication process was used to obtain a good dispersion solution. The substrate in this work was an aluminum metal sheet. Before use, the substrate was cleaned with deionized water, acetone, methanol, isopropanol in an ultrasonic bath for 15 min per cleaning agent. Next, an electrostatic spinning process was applied to prepare the nanofibers of PMMA and FLG. Figure 1(a) depicts the schematic setup of the electrostatic spinning system. The precursor flow rate preparation conditions, the distance between nozzle and substrate, substrate temperature, high voltage, and a deposition time were kept at 3.5 ml/h, 40 mm, 120°C, 7 kV, and 5 min, respectively. Figure 1(b) demonstrates the prepared nanofibers composited on a metal substrate size of 20 mm x 20 mm. It can be observed that the prepared sample exhibited smooth uniformity over the substrate. The active area of the prepared sample of corrosion testing was 10x10 mm^2. In addition, the large area of sample can be prepared by the modified substrate stage.

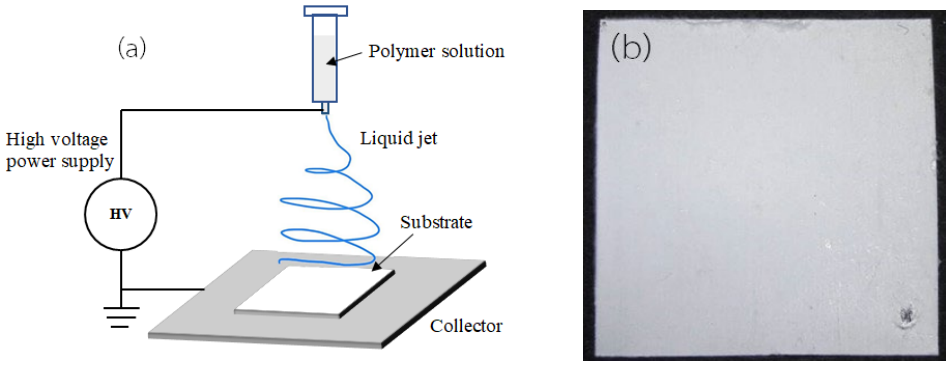

Figure 1. (a) Schematic setup of an electrospinning deposition system to prepare PMMA composited FLG nanofibers, (b) sample of prepared PMMA composited FLG nanofibers on 10 mm x 10 mm metal substrate

2.2 Materials characterization

The properties of the prepared nanofibers were characterized by field-emission scanning electron microscope (FE-SEM, JSM-7001F), Raman spectroscopy (DXR smart Raman), and lab-made contact angle measurement. A potentiostat (Autolab PGSTAT306, Metrohm) was used to evaluate the electrochemistry of the prepared samples as the working electrode. Corrosion testing was performed by immersing the working electrode in an aqueous solution of 3.5% by weight of NaCl. The reference and counter electrodes were Ag/AgCl and platinum sheet electrodes, respectively. Tafel measurements were undertaken to indicate the corrosion behavior of the prepared samples. Moreover, an equivalent circuit model was performed with electrochemical impedance spectroscopy to describe the anticorrosion mechanism.

3. Results and Discussion

Morphology images of the prepared nanofibers are shown in Figure 2. The insets in each picture exhibit the diameter distributions of nanofibers from 20 points of direct estimation. It was found that the composite nanofibers of FLG and PMMA were successively fabricated on the metal substrates. It can be seen that the diameters of nanofibers decreased when increasing the content of FLG. The mean diameters of the nanofibers were 1.37, 0.81, 0.49, and 0.47 μm for pristine PMMA, 0.2, 0.5, and 2% by weight of FLG, respectively. Generally, the physical properties of NFs prepared by the electrospinning process depend on the properties of precursor solution such as viscosity [22]. Differences in composition of FLG in PMMA solutions result in different properties of the mixing solution that was used as precursor solution. Moreover, the interlacing of nonwoven composited NFs can enhance the waterproofing and hydrophobic properties [23], which are factors of importance for corrosion inhibitor materials.

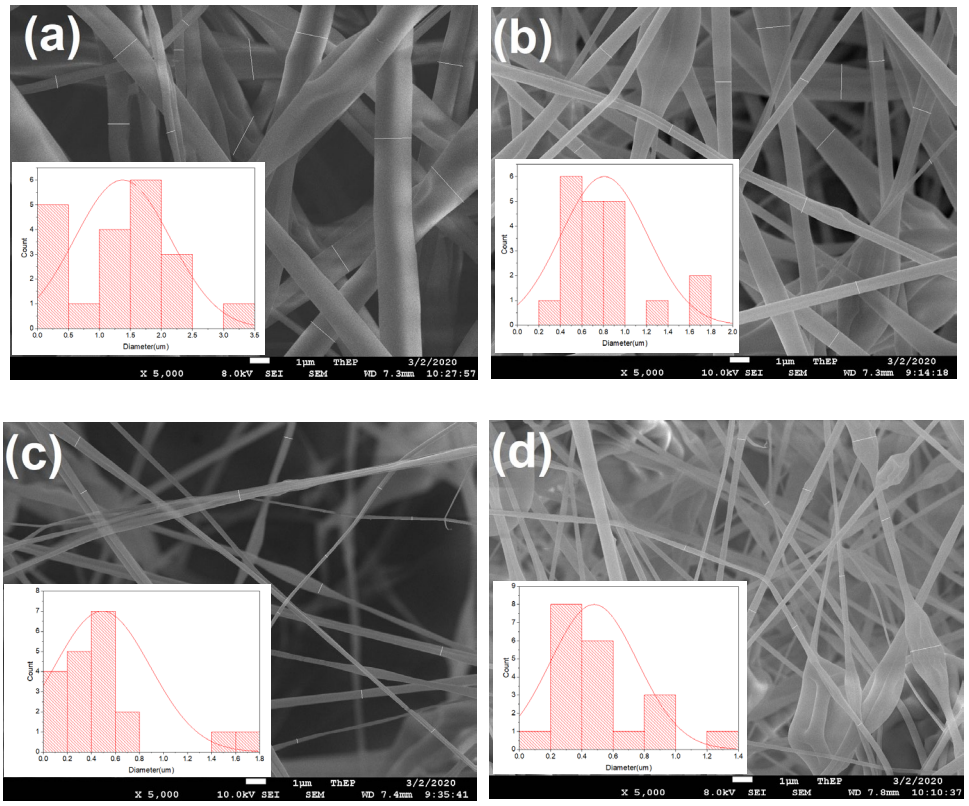

Figure 2. Morphology images of (a) PMMA NFs, (b) 0.2 wt%, (c) 0.5%, and (d) 2 wt% of FLG-PMMA NFs. The insets exhibited the diameter distribution of nanofibers.

The Raman spectroscopy is a typical instrument [24] which was used to assess the electronic and vibrational characteristics of carbon-based materials. The Raman spectra in the wavenumber range of 1100 to 2200 cm^{-1} of the prepared nanofibers are shown in Figure 3. The spectra of pristine PMMA nanofibers exhibited two peaks, at 1456 and 1736 cm^{-1}, which can be

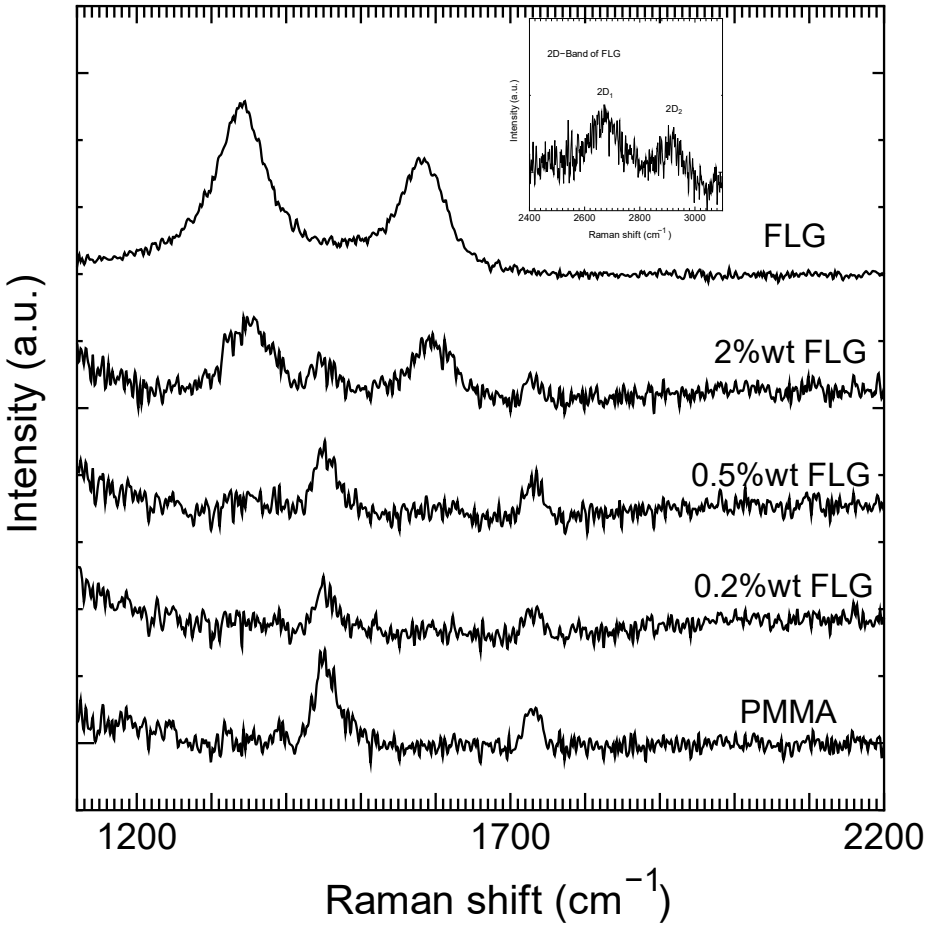

Figure 3. Raman spectra of pristine FLG powder, PMMA nanofibers, and PMMA composited FLG nanofibers (inset: the 2D band of FLG)

attributed to δ_a (C–H) of α-CH_3, δ_a(C–H) of O–CH_3, and ν(C=O) of (C–COO) [25], respectively. The spectra of pristine FLG powder exhibited the D-band and the G-band at the wavenumbers of 1342 and 1580 cm^{-1}, respectively. It is well known that the G-band is a Raman active mode due to the sp^2 bonding of carbon atoms in graphene structure, whereas the D-band is a defect band of graphene structure [26]. The intensity ratio of D-band and G-band (I_D/I_G) was 1.43, which indicated the reduced graphene oxide. The number of layers of FLG can be estimated with Raman spectra [27] with the intensity of $2D_1$ peaks of Raman spectra at 2700 cm^{-1}, as shown in the inset of Figure 3. It was found that the intensity ratio of $2D_1$/G peaks was about 0.12; this indicated more than three stacking layers in the graphene flakes. In the case of composited NFs with a low concentration of FLG (0.2 and 0.5 wt%), the spectra showed Raman characteristics of PMMA material, predominantly. This may have been due to embedded FLG in PMMA host material. However, in the case of a higher concentration (2 wt%), the Raman characteristic of FLG was observed as G- and D- bands, while the spectral peaks of PMMA still occurred. These results confirmed that the composite FLG and PMMA nanofibers had been fabricated.

Typically, the wettability of the surface is an important parameter that can affect the corrosion properties of a material. Normally, a corrosion inhibitor's function depends on its protective coating characteristics such as water absorption, water transport, and water accessibility [28]. The surface contact angle of composited nanofibers was determined in our laboratory. One drop of 1 microliter deionized water was fed by micropipette onto the composited nanofiber surface. A digital microscope with 1000x magnification was used to record images, which are shown in Figure 4. The contact angle was calculated from a direct estimation of measurement images. It can be seen that the contact angle increased when increasing the concentration of FLG in composited nanofibers with contact angles of 121.70, 125.53, 124.99, and 127.87 degrees for pristine PMMA NFs, 0.2, 0.5, and 2wt% of FLG in PMMA NFs, respectively. Therefore, the hydrophobic behavior was greater in the case of higher content of FLG material. Chang *et al*. [28] reported the anticorrosion properties of the hydrophobic surface of epoxy/graphene composites. So, the hydrophobic surfacing diminished the absorption of moisture and ions into the composited material, which inhibited corrosion behavior.

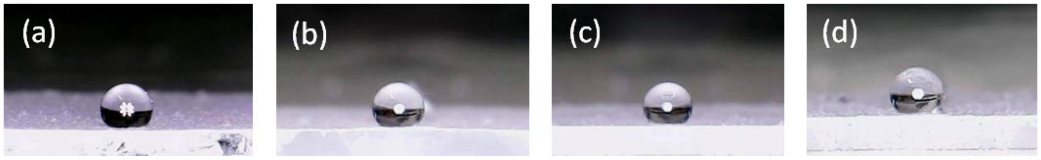

Figure 4. Surface contact angle of (a) PMMA NFs, (b) 0.2 wt%, (c) 0.5 wt %, and (d) 2 wt% of FLG-PMMA NFs

Electrochemical measurement was applied to evaluate the anticorrosion behavior of the prepared samples. The Tafel plot is a common method used to estimate corrosion parameters. Figure 5 depicts the Tafel plot of samples in 3.5% saline aqueous solution with electrode current density in logarithm scale. It can be seen that the coated samples demonstrate a more positive corrosion potential than the bare Al metal. The shift of current density to a lower value can be indicated by increasing anticorrosion behavior in the prepared samples. With the Tafel plot, the corrosion current (I_{corr}) and corrosion potential (E_{corr}) can be obtained by extrapolating straight line of oxidation and reduction process in the Tafel graph. The inset in Figure 5 depicts the extrapolating of the Tafel plot to obtain the I_{corr} and E_{corr}. To indicate the performance of the prepared sample, the corrosion protection efficiency (P.E. (%)) was calculated as follows [14] :

$$P.E.(\%) = \frac{I^0_{corr} - I^c_{corr}}{I^0_{corr}} \times 100 \quad (1)$$

Where I^0_{corr} is the corrosion current of the metal substrate, and I^c_{corr} is the corrosion current of the prepared sample.

The parameters of the anticorrosion measurement that were evaluated from the Tafel plot are shown in Table 1. It was found that there was a positive increase of E_{corr} in the composited NFs compared with the Al pure metal and PMMA NFs, respectively. Therefore, it was concluded that the composited NFs could be used to prevent the current flow through the samples, which is a behavior of anticorrosion inhibitors. The maximum corrosion protection efficiency was 99.33% in 2.0 wt% FLG composites PMMA NFs compared with the bare Al metal. It can be seen that the corrosion protection efficiency demonstrated the performance of the anticorrosion properties of composite FLG and PMMA NFs, a result which is consistent with other literature [12-14, 28]. However, Hao *et al*. [29] reported a higher composited concentration of the materials poly N-

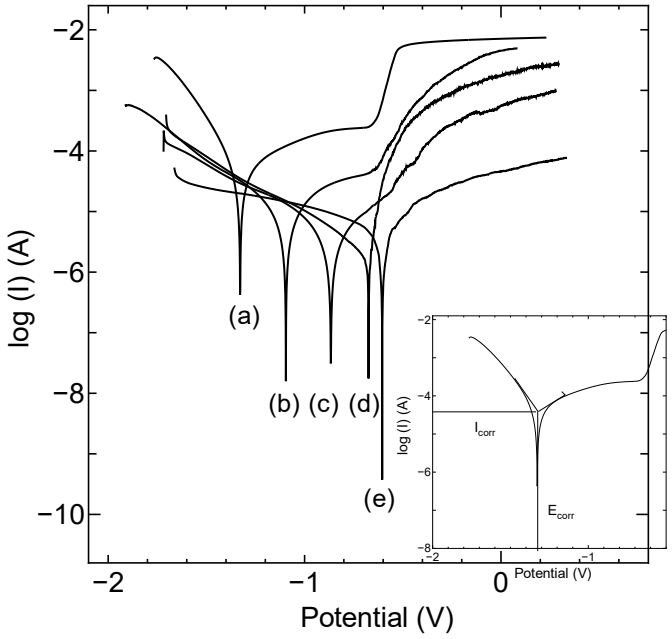

Figure 5. Tafel plots of (a) bare Al substrate sheet, (b) PMMA NFs, (c) 0.2 wt% FLG-PMMA NFs, (d) 0.5 wt% FLG-PMMA NFs, and (e) 2 wt% FLG-PMMA in 3.5wt% NaCl aqueous solutions. (Inset: the E_{corr} and I_{corr} of Tafel plots)

Table 1. Electrochemical parameters of PMMA composited with FLG for anticorrosion protective layers derived from the Tafel plot

Sample	Icorr (A/cm^2)	Ecorr (vs. Ag/AgCl) (V)	P.E. (%)
Bare Al	58.702 x 10^{-6}	-1.327	-
PMMA	11.633 x 10^{-6}	-1.102	80.18
0.2	3.602 x 10^{-6}	-0.864	93.86
0.5	1.907 x 10^{-6}	-0.662	96.75
2	0.390 x 10^{-6}	-0.605	99.33

(vinyl)pyrrole and carbon black. When the carbon black was increased, ane increased corrosion current was observed due to the excess of carbon black inside the polymer. This behavior can be seen in other composite materials such as polyaniline/clinoptilolite nanocomposite, cerium oxide-graphene oxide, and multiwall carbon nanotubes-reinforced epoxy [30-32].

Electrochemical impedance spectroscopy is a technique that had been widely used to investigate the mechanisms of electrochemical applications [4]. The Cole-Cole plot of composite FLG in PMMA NFs in the frequency range of 1 to 1x10 ^{5} Hz is shown in Figure 6(a), which displays the real part (Z') and imaginary part (Z") of sample impedance plotted as the x-axis and y-axis, respectively. The behavior of charge carriers at the working electrode was represented in terms of impedance value. The impedance characteristics exhibited a semicircle shape in this graph, which also had a linear tail at high frequency. To better explain the results, an equivalent circuit model of the working electrode is shown in Figure 6(b) [14], which was composed of the essential electronic

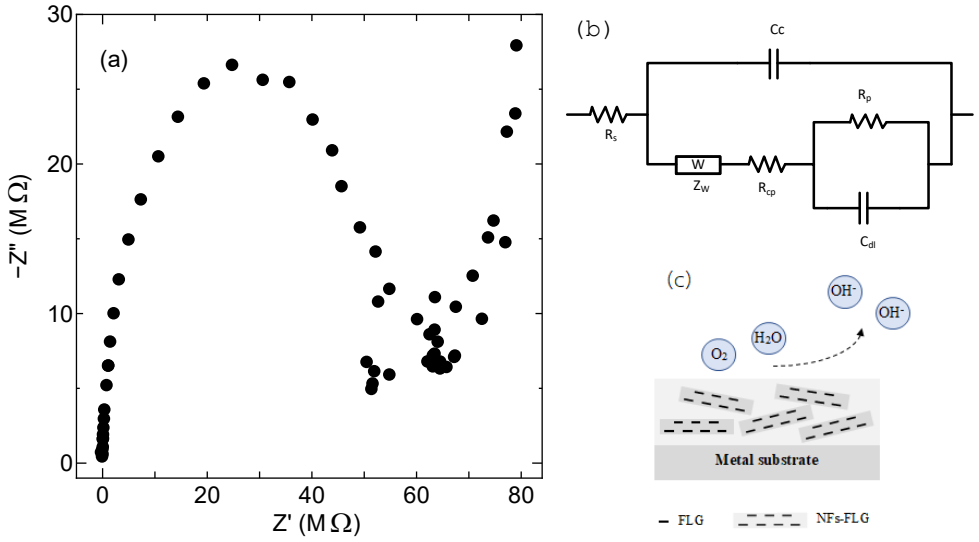

Figure 6. (a) Cole-Cole plot of composited NFs, (b) an equivalent circuit model of prepared NFs, and (c) proposed mechanism model of anticorrosion

elements, including resistance and capacitance. In the circuit model, R_s, C_c, Z_w, R_{cp}, R_p, and C_{dl} represent the electrolyte resistance, the coating capacitance, the Warburg component, the pore resistance of the NFs coating, the polarization resistance, and the electric double-layer capacitor, respectively. In addition, Figure 6c depicts the proposed anticorrosion mechanism diagram of composite NFs [33]. Due to the corrosion process in aqueous chloride solution being an anodic process of the Al metal, the chemical reaction of O_2 and H_2O is required for the corrosion process on the metal surface. For this reason, the main mode of action of the anticorrosion layer is to prevent the diffusion of aqueous ions to the metal substrate. In the composite nanofibers, the diffusion pathways of oxygen and water molecules to the substrate increased when compared with only the bare metal substrate. Both the tortuous path of composite FLG in PMMA nanofiber and the hierarchical structures of nanofibers might reduce the reach of aqueous ions on the metal substrate/electrolyte interface. Typically, the gas permeability of composite materials decreases due to the increase of tortuosity that decreases the permeability of ions and gases in the composite layer [1, 34]. Therefore, the current flow in the prepared sample related to the corrosion behavior was reduced. Thus, the composite FLG and PMMA NF can be used as corrosion inhibitors [35].

4. Conclusions

A nanofiber anticorrosion layer of poly (methyl methacrylate) (PMMA) composited with few-layer-graphene (FLG) was successfully prepared using the electrospinning process. The physical properties of morphology, Raman scattering, and surface contact angle of the prepared nanofibers were investigated. The electrochemical properties of the prepared nanofibers were measured in an aqueous solution of 3.5% by weight of sodium chloride. The Tafel plot of the prepared sample was used to indicate the anticorrosion performance of the PMMA: FLG NFs. The optimum corrosion protection efficiency was found in the sample of 2 wt% of FLG in PMMA, with an efficiency value of 99.33%. The mechanism of anticorrosion behavior of prepared NFs was investigated by

electrochemical impedance spectroscopy. The composited NF acted as a corrosion inhibitor due to the increase of the diffusion of oxygen and water molecules to the metal substrate.

5. Acknowledgments

This work was financially supported by King Mongkut's Institute of Technology Ladkrabang (KMITL) research fund (RE-KRIS/FF65/39). The authors acknowledge the facilities and technical assistance from Nanotechnology and Materials Analytical Instrument Service Unit (NMIS) of College of Materials Innovation and Technology, King Mongkut's Institute of Technology Ladkrabang.

References

[1] Chang, C.H., Huang, T.C., Peng, C.W., Yeh, T.C., Lu, H.I., Hung, W.I., Weng, C.J., Yang, T.I. and Yeh, J.M., 2012. Novel anti-corrosion coatings prepared from polyaniline/graphene composites. *Carbon*, 50 (14), 5044-5051.

[2] Oyekunle, D.T., Agboola, O. and Ayeni, A.O., 2019. Corrosion Inhibitors as Building Evidence for Mild Steel: A Review. *Journal of Physics: Conference Series*, 1378(3), 032046, https://doi.org/10.1088/1742-6596/1378/3/032046.

[3] Verma, C., Ebenso, E.E., Bahadur, I. and Quraishi, M.A., 2018. An overview on plant extracts as environmental sustainable and green corrosion inhibitors for metals and alloys in aggressive corrosive media. *Journal of Molecular Liquids,* 266, 577-590.

[4] Meng, Y., Liu, L., Zhang, D., Dong, C., Yan, Y., Volinsky, A.A. and Wang, L.N., 2019. Initial formation of corrosion products on pure zinc in saline solution. *Bioactive Materials*, 4, 87-96.

[5] Prasai, D., Tuberqui, J.C., Harl, R.R., Jennings, G.K. and Bolotin, K.I., 2012. Graphene: Corrosion-Inhibiting Coating. *ACS Nano*, 6(2), 1102-1108.

[6] Kear, G., Barker, B.D., Stokes, K. and Walsh, F.C., 2004. Electrochemical Corrosion Behaviour of 90—10 Cu—Ni Alloy in Chloride-Based Electrolytes. *Journal of Applied Electrochmistry*, 34, 659-669.

[7] Tsai, S.-T., ChangJean, W.-C., Huang, L.-Y. and Tsai, T.-C., 2020. On the anti-corrosion property of dry-gel-conversion-grown MFI zeolite coating on aluminum alloy. *Materials*, 13(20), 4595, https://doi.org/10.3390/ma13204595.

[8] Craciun, M.F., Khrapach, I., Barnes, M.D. and Russo, S., 2013. Properties and applications of chemically functionalized graphene. *Journal of Physics: Condensed Matter*, 25(42), 423201, https:/doi.org1088/0953-8984/25/42/423201/.

[9] Kim, H., Miura, Y. and Macosko, C.W., 2010. Graphene/polyurethane nanocomposites for improved gas barrier and electrical conductivity. *Chemistry of Materials*, 22(11), 3441-3450.

[10] Aïssa, B., Memon, N., Ali, A. and Khraisheh, K., 2015. Recent progress in the growth and applications of graphene as a smart material: a review. *Frontiers in Materials*, 2, 58, https://doi.org/10.3389/fmats.2015.0058.

[11] Rajabi, M., Rashed, G.R. and Zaarei, D., 2014. Assessment of graphene oxide/epoxy nanocomposite as corrosion resistance coating on carbon steel. *Corrosion Engineering, Science and Technology,* 50(7), 509-516.

[12] Krishnan, M.A., Aneja, K.S., Shaikh, A., Bohm, S., Sarkar, K., Bohm, H.L. and Raja, V.S., 2018. Graphene-based anticorrosive coatings for copper. *RSC Advances*, 8(1), 499-507.

[13] Chen, S., Brown, L., Levendorf, M., Cai, W., Ju, S.Y., Edgeworth, J., Li, X., Magnuson, C.W., Velamakanni, A., Pine, R.D., Kang, J., Park, J. and Ruoff, R.S., 2011. Oxidation resistance of graphene-coated Cu and Cu/Ni alloy. *ACS Nano*, 5(2), 1321-1327.

[14] Yu, Y.H., Lin, Y.Y., Lin, C.H., Chan, C.C. and Huang, Y.C., 2014. High-performance polystyrene/graphene-based nanocomposites with excellent anti-corrosion properties. *Polymer Chemistry*, 5(2), 535-550.

[15] Bohm, S., 2014. Graphene against corrosion, *Nature Nanotechnology*, 9(10), 741-742.

[16] Agarwal, S., Greiner, A. and Wendorff, J.H., 2013. Functional materials by electrospinning of polymers. *Progress in Polymer Science*, 38(6), 963-991.

[17] Ding, B., Wang, M., Wang, X., Yu, J. and Sun, G., 2010. Electrospun nanomaterials for ultrasensitive sensors. *Materialstoday*, 13(11), 16-27.

[18] Liang, J., Zhao, H., Yue, L., Fan, G., Li, T., Lu, S., Chen, G., Gao, S., Asiri, A.M. and Sun, Z., 2020. Recent advances in electrospun nanofibers for supercapacitors. *Journal of Materials Chemistry A*, 8(33), 16747-16789.

[19] Jiang, S., Schmalz, H., Agarwal, S. and Greiner, A., 2020. Electrospinning of ABS nanofibers and their high filtration performance. *Advanced Fiber Materials*, 2, 34-43.

[20] Ju, B.J., Oh, J.H., Yun, C. and Park, C.H., 2018. Development of a superhydrophobic electrospun poly(vinylidene fluoride) web via plasma etching and water immersion for energy harvesting applications. *RSC Advances*, 8, 28825-28835.

[21] Hashim, A. and Abbas, B., 2019. Recent review on Poly-methyl methacrylate (PMMA)-polystyrene (PS) blend doped with nanoparticles for modern applications. *Research Journal of Agriculture and Biological Sciences*, 14(3), 6-12.

[22] Abdelsamad, A.M.A., Kwankhao, B., Gad-Allah, T.A., Khalil, A.S.G., Badawy, M.I., Bahners, T. and Ulbricht, M., 2017. Hydrophilic polyethersulfone-based microfiltration membranes by electrospinning of polymer blends. *Desalination and Water Treatment*, 86, 89-95.

[23] Yu, Y., Zhang, F., Liu, Y., Zheng, Y., Xin, B., Jiang, Z., Peng, X. and Jin, S., 2020. Waterproof and breathable polyacrylonitrile/(polyurethane/fluorinated-silica) composite nanofiber membrane via side-by-side electrospinning. *Journal of Materials Research*, 35(9), 1173-1181.

[24] Gurbani, N., Han, C.P., Marumoto, K., Liu, R.S., Choudhary, R.J. and Chouhan, N., 2018. Biogenic reduction of graphene oxide: An efficient superparamagnetic material for photocatalytic hydrogen production. *ACS Applied Energy Materials*, 1(11), 5907-5918.

[25] Thomas, K.J., Sheeba, M., Nampoori, V.P.N., Vallabhan, C.P.G. and Radhakrishnan, P., 2008. Raman spectra of polymethyl methacrylate optical fibres excited by a 532 nm diode pumped solid state laser. *Journal of Optics A: Pure and Applied Optics*, 10, 055303, https://doi.org/10.1088/1464-4258/10/5/055303.

[26] Cançado, L.G., Jorio, A., Ferreira, E.H.M., Stavale, F., Achete, C.A., Capaz, R.B., Moutinho, M.V.O., Lombardo, A., Kulmala, T.S. and Ferrari, A.C., 2011, Quantifying defects in graphene via Raman spectroscopy at different excitation energies. *Nano Letters*, 11(8), 3190-3196.

[27] Das, A., Chakraborty, B. and Sood, A.K., 2008. Raman spectroscopy of graphene on different substrates and influence of defects. *Bulletin of Materials Science*, 31, 579-584.

[28] Chang, K.C., Hsu, M.H., Lu, H.I., Lai, M.C., Liu, P.J., Hsu, C.H., Ji, W.F., Chuang, T.L., Wei, Y., Yeh, J.M. and Liu, W.R., 2014. Room-temperature cured hydrophobic epoxy/ graphene composites as corrosion inhibitor for cold-rolled steel. *Carbon*, 66, 144-153.

[29] Hao, L., Lv, G., Zhou, Y., Zhu, K., Dong, M., Liu, Y. and Yu, D., 2018. High performance anti-corrosion coatings of poly (vinyl butyral) composites with poly N-(vinyl)pyrrole and carbon black nanoparticles. *Materials*, 11(11), 2307, https://doi.org/10.3390/ma11112307.

[30] Olad, A. and Naseri, B., 2010. Preparation, characterization and anticorrosive properties of a novel polyaniline/clinoptilolite nanocomposite. *Progress in Organic Coatings*, 67(3), 233-238.

[31] Liu, X., Jie, H., Liu, R., Liu, Y., Li, T. and Lyu, K., 2021. Research on the preparation and anticorrosion properties of EP/CeO_2-GO nanocomposite coating. *Polymers*, 13(2), 183, https://doi.org/10.3390/polym13020183.

[32] Shen, W., Feng, L., Liu, X., Luo, H., Liu, Z., Tong, P. and Zhang, W., 2016. Multiwall carbon nanotubes-reinforced epoxy hybrid coatings with high electrical conductivity and corrosion resistance prepared via electrostatic spraying. *Progress in Organic Coatings*, 90, 139-146.

[33] Necolau, M.I. and Pandele, A.M., 2020. Recent advances in graphene oxide-based anticorrosive coatings: An overview. *Coating*, 10, 1149, https://doi.org/10.3390/coatings 10121149.

[34] Huang, H.D., Ren, P.G., Chen, J., Zhang, W.Q., Ji, X. and Li, Z.M., 2012. High barrier graphene oxide nanosheet/poly(vinyl alcohol) nanocomposite films. *Journal of Membrane Science*, 409-410, 156-163.

[35] Ghauri, F.A., Raza, M.A., Baig, M.S. and Ibrahim, S., 2017. Corrosion study of the graphene oxide and reduced graphene oxide-based epoxy coatings. *Material Research Express*, 4(12), 125601, https://doi.org/10.1088/2053-1591/aa9aac.